ACS OMEGA

http://pubs.acs.org/journal/acsodf

Article

Combined Multiomics and In Silico Approach Uncovers PRKAR1A as a Putative Therapeutic Target in Multi-Organ Dysfunction Syndrome

Prithvi Singh, Mohd Mohsin, Armiya Sultan, Prakash Jha, Mohd Mabood Khan, Mansoor Ali Syed, Madhu Chopra, Mohammad Serajuddin, Arshad Husain Rahmani, Saleh A. Almatroodi, Faris Alrumaihi, and Ravins Dohare*

Cite This: *ACS Omega* 2023, 8, 9555−9568

Read Online

ACCESS | Metrics & More | Article Recommendations | Supporting Information

ABSTRACT: Despite all epidemiological, clinical, and experimental research efforts, therapeutic concepts in sepsis and sepsis-induced multi-organ dysfunction syndrome (MODS) remain limited and unsatisfactory. Currently, gene expression data sets are widely utilized to discover new biomarkers and therapeutic targets in diseases. In the present study, we analyzed MODS expression profiles (comprising 13 sepsis and 8 control samples) retrieved from NCBI-GEO and found 359 differentially expressed genes (DEGs), among which 170 were downregulated and 189 were upregulated. Next, we employed the weighted gene co-expression network analysis (WGCNA) to establish a MODS-associated gene co-expression network (weighted) and identified representative module genes having an elevated correlation with age. Based on the results, a turquoise module was picked as our hub module. Further, we constructed the PPI network comprising 35 hub module DEGs. The DEGs involved in the highest-confidence PPI network were utilized for collecting pathway and gene ontology (GO) terms using various libraries. Nucleotide di- and triphosphate biosynthesis and interconversion was the most significant pathway. Also, 3 DEGs within our PPI network were involved in the top 5 significantly enriched ontology terms, with hypercortisolism being the most significant term. PRKAR1A was the overlapping gene between top 5 significant pathways and GO terms, respectively. PRKAR1A was considered as a therapeutic target in MODS, and 2992 ligands were screened for binding with PRKAR1A. Among these ligands, 3 molecules based on CDOCKER score (molecular dynamics simulated-based score, which allows us to rank the binding poses according to their quality and to identify the best pose for each system) and crucial interaction with human PRKAR1A coding protein and protein kinase-cyclic nucleotide binding domains (PKA RI alpha CNB-B domain) via active site binding residues, viz. Val283, Val302, Gln304, Val315, Ile327, Ala336, Ala337, Val339, Tyr373, and Asn374, were considered as lead molecules.

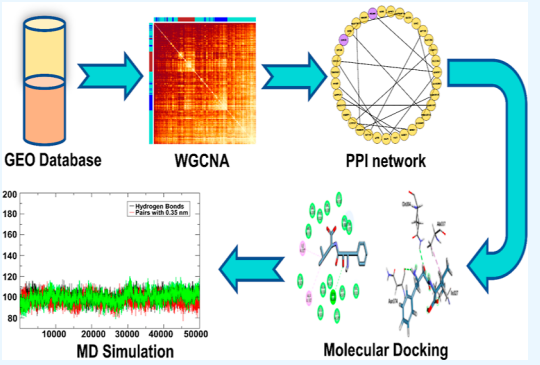

1. INTRODUCTION

One of the oldest elusive syndromes is sepsis. The term "sepsis" describes the syndrome of infection intricated by acute organ dysfunction.[1] When sepsis is not clinically detected and managed at an earlier stage, it contributes to the advancement of septic shock and multiple organ failure, eventually leading to death.[2] Patients with severe infectious diseases such as lower respiratory and diarrheal diseases are at a higher risk of developing and dying from sepsis.[3] Septic patients frequently develop multiple organ failures, particularly during the treatment in critical care units of hospitals.[4] This newly developed clinical condition prolongs the recovery of sepsis patients, contributing to heightened morbidity and mortality worldwide.[5,6] It is anticipated that about 49×10^6 people are affected and approximately 11×10^6 global fatalities occur due to sepsis every year.[3]

Immediate diagnosis of sepsis is crucial to protect patients from sepsis-related complications and to provide well-timed treatment. Currently, in-use biomarkers for the diagnosis of sepsis include C-reactive protein, procalcitonin, and interleukin-6.[7] However, these biomarkers have been reported to carry less specificity and cannot diagnose sepsis at an earlier stage.[8] Therefore, researchers are devoted to discovering new biomarkers for the initial diagnosis and well-timed treatment of sepsis. Some studies have discovered that serum expression levels of soluble urokinase plasminogen activator receptor,[9] presepsin,[10] soluble triggering receptor,[11] and CD64[12] are upregulated in sepsis patients. Many recent studies have highlighted microRNAs (miRNAs),[13,14] long noncoding RNAs,[15] and microbiome[16] as emerging interests in recognizing and advancing new biomarkers in sepsis. However, such efforts

Received: January 2, 2023
Accepted: February 20, 2023
Published: March 1, 2023

have not yet resulted in a satisfactory outcome for diagnosing and treating sepsis and sepsis-related multi-organ dysfunction.

Sepsis in its severe form has been reported to be linked with several critical complications such as coagulopathy,[17] immunosuppression,[18] persistent inflammation,[19] immunosuppression and catabolism syndrome,[20] acute respiratory distress syndrome,[21,22] acute kidney injury,[23] systemic lupus erythematosus,[24] and cardiac dysfunction.[25] Cardiac dysfunction and acute kidney injury are the two most prevalent independent risk factors responsible for increased mortality rate in sepsis syndrome.[26] Overrunning and unregulated responses from the host immune system toward a severe form of sepsis can cause critical organ tissue injuries, contributing to irreversible organ failure.[19,27] The failure of dual or additional important organ systems is known as multi-organ dysfunction syndrome (MODS). Sepsis-induced MODS is raised as a critical complication contributing to high morbidity and mortality.[28]

Despite all epidemiological, clinical, and experimental research efforts, therapeutic concepts in sepsis and sepsis-induced MODS remain limited and unsatisfactory. Evidence-based therapy for sepsis still resides on basic causal and supportive measures. Adjuvant interventions, including targeted immunotherapy, still lack proof of effectiveness so far.[4] Importantly, no treatment strategy is available to counteract the MODS development during sepsis effectively. Therefore, the Surviving Sepsis Campaign (SSC) was started comprehensively in 2004 to advance the global treatment of sepsis and sepsis-related complications.[29] SSC is a joint initiative of the Society of Critical Care Medicine (SCCM) and the European Society of Intensive Care Medicine (ESICM), which are committed to reducing mortality and morbidity from sepsis and septic shock worldwide[30] (https://www.sccm.org/SurvivingSepsisCampaign/Home).

Bioinformatics-based approaches are widely used tools to explore, research, understand, and describe human health's structural and relational qualities and health-related ailments.[31−33] Bioinformatics analysis is emerging as a crucial tool to determine the vulnerability of molecular markers associated with diseases and significantly contributes to system pharmacology. It offers an ideal way to screen large gene expression data sets to comprehensively understand the molecular and biochemical processes associated with underlying diseases. Researchers are globally making efforts to identify new biomarkers and therapeutic targets from large gene expression data sets for early diagnosis and well-timed treatment of diseases. Bioinformatics-based analysis of disease-associated data sets has comprehensively discovered many new drug targets in several diseases.[32−37] In the present study, we integrated sepsis-related data sets and used in silico bioinformatics analysis to discover the differentially expressed genes (DEGs) involved in sepsis and sepsis-induced MODS. The National Center for Biotechnology Information (NCBI)-Gene Expression Omnibus (GEO) was accessed to extract MODS-associated mRNA expression profiles followed by MODS-associated weighted gene co-expression network (WGCN) formation to identify representative module genes having a superior correlation with sample clinical characteristics. Molecular mechanisms underlying the sepsis and sepsis-induced MODS were also explored to discover novel treatment targets. Following that, various structural biology methods were utilized to screen and discover lead compounds with possible repressing effects on the identified target gene, including virtual screening, molecular docking, and so on. This research identifies a potential new treatment for sepsis-induced MODS.

2. MATERIALS AND METHODS

2.1. Microarray Data Collection and Differential Expression Analysis. NCBI-GEO[38] (https://www.ncbi.nlm.nih.gov/geo/) was accessed to extract MODS-associated messenger RNA (mRNA) expression profiles with "MODS" and "Multiple Organ Dysfunction Syndrome" being used as keywords. The inclusion and exclusion criteria set for selecting appropriate data sets are mentioned in the Supporting Information. The expression file (series matrix format) of the chosen data set was extracted utilizing the GEOquery package. Probe ID mapping to their corresponding HUGO Gene Nomenclature Committee (HGNC) symbols was handled using the official sequencing platform library-based R package corresponding to which the samples were sequenced. The gene expression values mapping to numerous probe IDs was averaged to prevent redundancy. *t*-test (two-sample) was utilized for computing the *p*-value of every gene among control and MODS samples followed by obtaining their Benjamini−Hochberg (BH) *p*-value and $\log_2$(fold change) utilizing the limma package.[39] All genes corresponding to BH-*p*-value < 0.01 and $|\log_2(\text{fold change})| > 1.5$ were regarded as DEGs. DEGs with $\log_2(\text{fold change}) > 1.5$ and $\log_2(\text{fold change}) < -1.5$ were branched as up- and downregulated, respectively.

2.2. MODS-Associated WGCN Formation and Hub Module Selection. The weighted gene co-expression network analysis (WGCNA) package[40] was employed to establish MODS-associated WGCN and identify vital module genes having an elevated correlation with age. The age data of patient samples were considered before identifying module(s). Correct soft-threshold power (β) in compliance with the scale-free topology (SFT) criterion was selected using the pickSoftThreshold function for adjacency computation. The adjacency matrix (weighted) was translated into a topological overlap matrix (TOM) for the decline in false associations and noise followed by corresponding dissimilarity (dissTOM) computation. A dendrogram of genes in compliance with dissTOM was produced utilizing the *hclust* function. Next, a dynamic tree cut algorithm was employed to reveal densely interconnected modules from the dendrogram branches. Module eigengenes (MEs) and dissimilarity measure (MEdiss) among MEs were computed to unify modules with elevated co-expressed genes. Correlation-based absolute module significance (GS) values with age of samples followed by module membership (MM) for all modules were computed. Intramodular connectivity (k.in) is a measure of network connectivity concerning nodes or genes of a specific module. Correlations of MM versus GS, GS versus k.in, and MM versus k.in were employed to choose our hub module.

2.3. Protein−Protein Interaction Network Construction, Pathway, and Functional Enrichment Analyses. Filtered DEGs (based on high GS and MM) from the hub module were entered into the Search Tool for the Retrieval of Interacting Genes (STRING, https://string-db.org/) v11.5 web-based tool[41] for the construction of protein−protein interaction (PPI) network at the highest confidence (equivalent to interaction score > 0.9) and visualized via Cytoscape v3.9.1.[42] The DEGs involved in the highest-confidence PPI network were used for collecting pathway and GO term enrichment data utilizing various libraries (i.e., BioPlanet, Reactome, WikiPathways for pathways, and Human Phenotype Ontology for GO

https://doi.org/10.1021/acsomega.3c00020
ACS Omega 2023, 8, 9555−9568

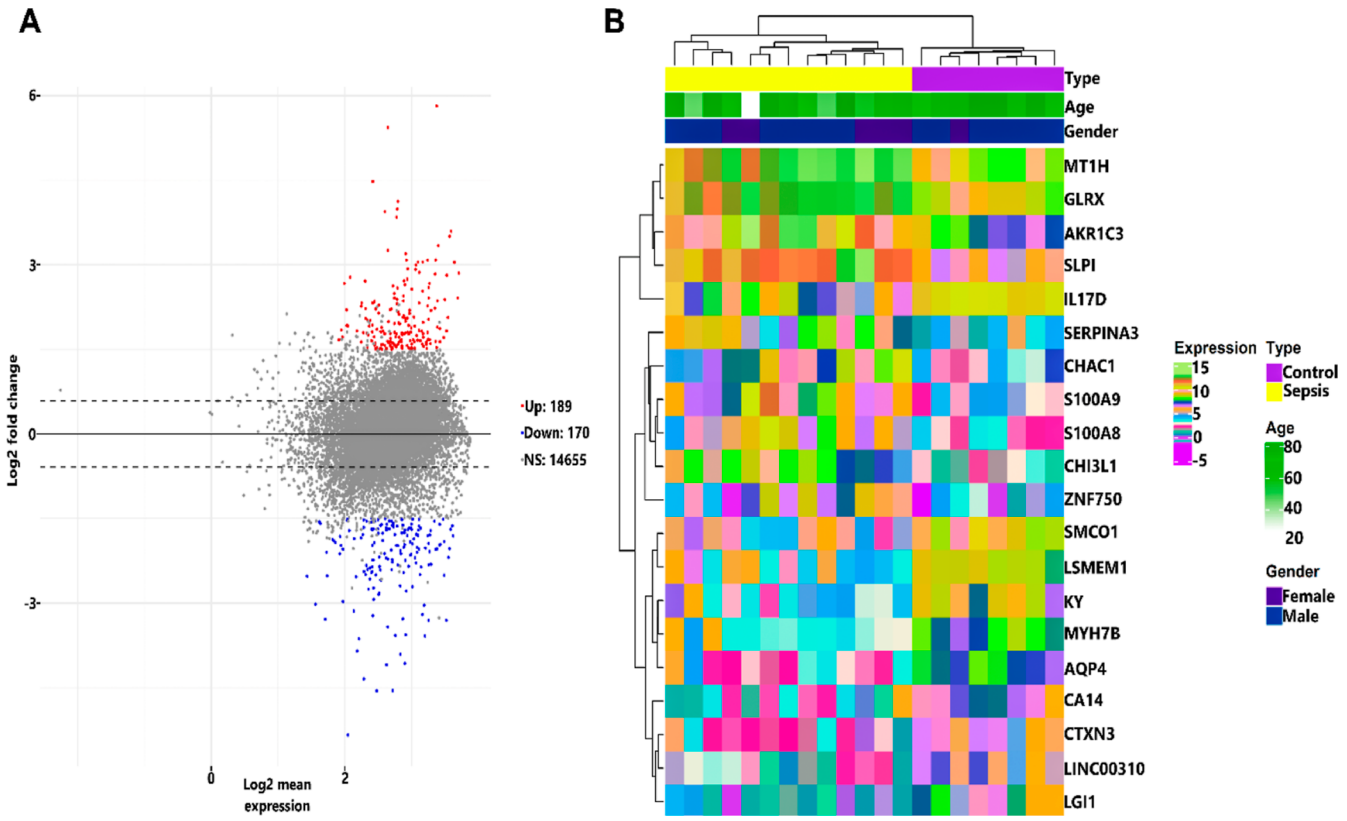

Figure 1. (A) MA plot demonstrating the disparity within expression values (mean) and fold change (log2) of 15,014 MODS genes. Red-, gray-, and blue-colored points signify upregulated (189), nonsignificant (14,655), and downregulated (170) genes, respectively. (B) Heatmap of top 10 down- and upregulated MODS-specific DEGs. Rows correspond to the normalized expression value of DEGs, and columns correspond to samples. The colored annotation bars representing the sample type (light magenta for controls and yellow for sepsis), gender type (dark magenta for females and dark blue for males), and age are positioned at the top of the heatmap.

term) within Enrichr database.[43,44] The top 5 pathways and GO terms corresponding to a p-value < 0.05 were regarded as statistically significant. Genes overlapping between these significant top 5 pathways and GO terms were considered as our hub gene(s).

2.4. Molecular Docking. We used the Food and Drug Administration (FDA)-approved library from Selleck Chem consisting of 2992 compounds for docking-based virtual screening. The 3D structures of these compounds were downloaded in the SDF format Selleck Chem database. Since the compounds were already FDA approved, there was no need for secondary filtration (Lipinski's Rule of 5, ADMET, and Topkat) of these compounds, and they could be directly employed for docking experiments. Next, these compounds were prepared, and energy was minimized by using the smart minimizer algorithm[45] available in Biovia DS 2020 for 5000 steps to attain an RMS gradient of 0.001. The human co-crystal structure of PKA RI alpha CNB-B domain with cAMP (PDB ID: 5KJX; Chain A)[46] was used as the target protein based on gene expression analysis. The protein structure was readied utilizing the protein preparation module of Biovia DS 2020 to add any missing residues, and hetatoms were also removed from the protein structure. The 3D coordinates were defined based on cAMP binding site, viz., $x = -2.18859$, $y = -3.24763$, and $z = 3.45037$. We utilized the LibDock docking algorithm of Biovia DS 2020 for high-throughput screening of the ligands followed by CDOCKER docking for accurate docking based on the molecular dynamics (MD) simulated docking algorithm using default parameters.[47]

2.5. MD Simulation. Using WebGro (https://simlab.uams.edu/), a GROMACS-based program, an MD simulation of the chosen molecules with the target protein PRKAR1A complex was carried out. The stability of the complexes was evaluated by looking at the root mean square deviation (RMSD), root mean square fluctuation (RMSF), radius of gyration (R_g), and intermolecular hydrogen binding. In order to perform MD simulation using the GROMOS96 43a1 forcefield, the topology for the best-fit model of the docked protein−ligand file was primarily prepared. Ligand topology parameters were produced using the open-source PRODRG server.[48] Our solvent model was SPC, and the complex was packed in a cubic box with a distance of 1 Å from the edges. Cl^- and Na^+ were added to neutralize the charge based on the overall charge. For energy minimization, the steepest descent algorithm with 5000 steps was used. The MD simulation was run in the presence of 0.15 M NaCl under NVT/NTP conditions (300 K, 1 bar). The number of cycles and simulation time for MD were both set to 50 ns.

3. RESULTS

3.1. Microarray Data Collection and Differential Expression Analysis. Based on the abovementioned inclusion criteria, we selected the MODS expression profile with GSE13205 as an accession identifier comprising 13 sepsis and 8 control patient samples. Probe IDs mapping to their equivalent HGNC symbols were done utilizing the hgu133plus2.db package. Post averaging the expression values equivalent to duplicates, we obtained 15,014 unique genes. A total of 359 genes were differentially expressed corresponding to BH-p-value

https://doi.org/10.1021/acsomega.3c00020
ACS Omega 2023, 8, 9555−9568

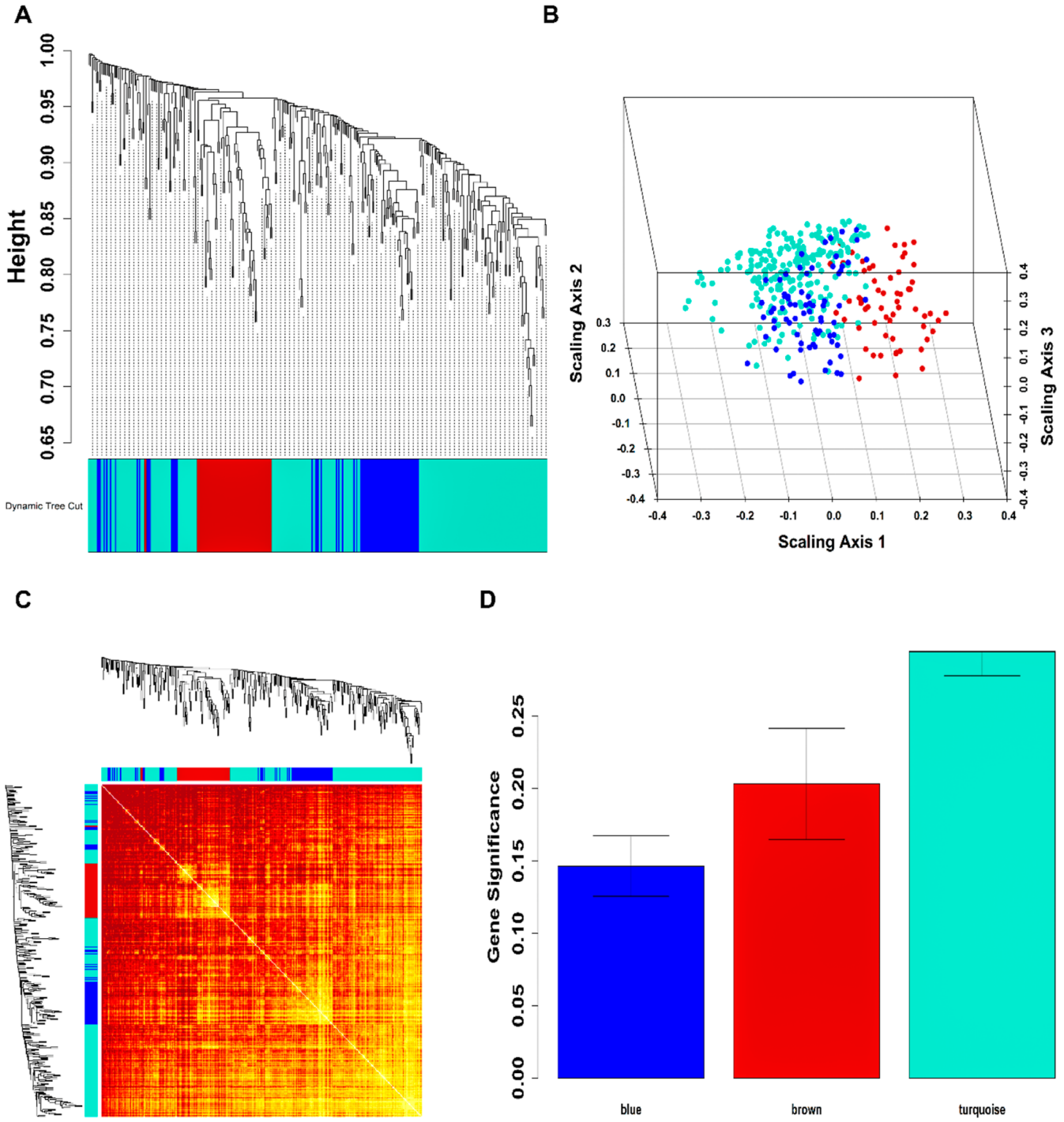

Figure 2. (A) Dendrogram of 359 MODS-associated DEGs clustered on the basis of disTOM and three communities (obtained using dynamic tree cut algorithm). (B) 3D MDS plot with every colored point signifying a gene fitting to a particular community of the corresponding color. (C) TOM plot of the WGCN signifying TOM among brown, blue, and turquoise community genes. The plot's top and left side panels represent hierarchically clustered gene dendrograms and module assignments. Dark-colored blocks along the diagonal represent communities. (D) Bar plot demonstrates the GS values distribution and error bars across blue, turquoise, and brown modules.

< 0.01 and $|\log_2(\text{fold change})| > 1.5$. Among all these DEGs, 170 were downregulated and 189 were upregulated as shown by the MA plot in Figure 1A. Within all the DEGs, LGI1 [$\log_2(\text{fold change}) = -5.34$] and SLPI [$\log_2(\text{fold change}) = 5.81$] had the highest fold change values across both scales. Figure 1B displays the expression heatmap of the top 10 down- and upregulated DEGs. The sample, age, and gender annotation bars are positioned at the top of the heatmap. The 8 control samples clustered distinctly from 13 sepsis samples as evidenced by the heatmap. Among all the samples, the majority of them were males (i.e., 71.4%) as compared to females (i.e., 28.6%).

3.2. MODS-Associated WGCN Construction and Hub Module Selection. All 359 MODS-associated DEGs were loaded with sample age information. $\beta = 12$ was chosen (equivalent to scale-free $R^2 = 0.80$) for the construction of a WGCN. Figure S1A–D shows plots for β in consideration of

https://doi.org/10.1021/acsomega.3c00020
ACS Omega 2023, 8, 9555−9568

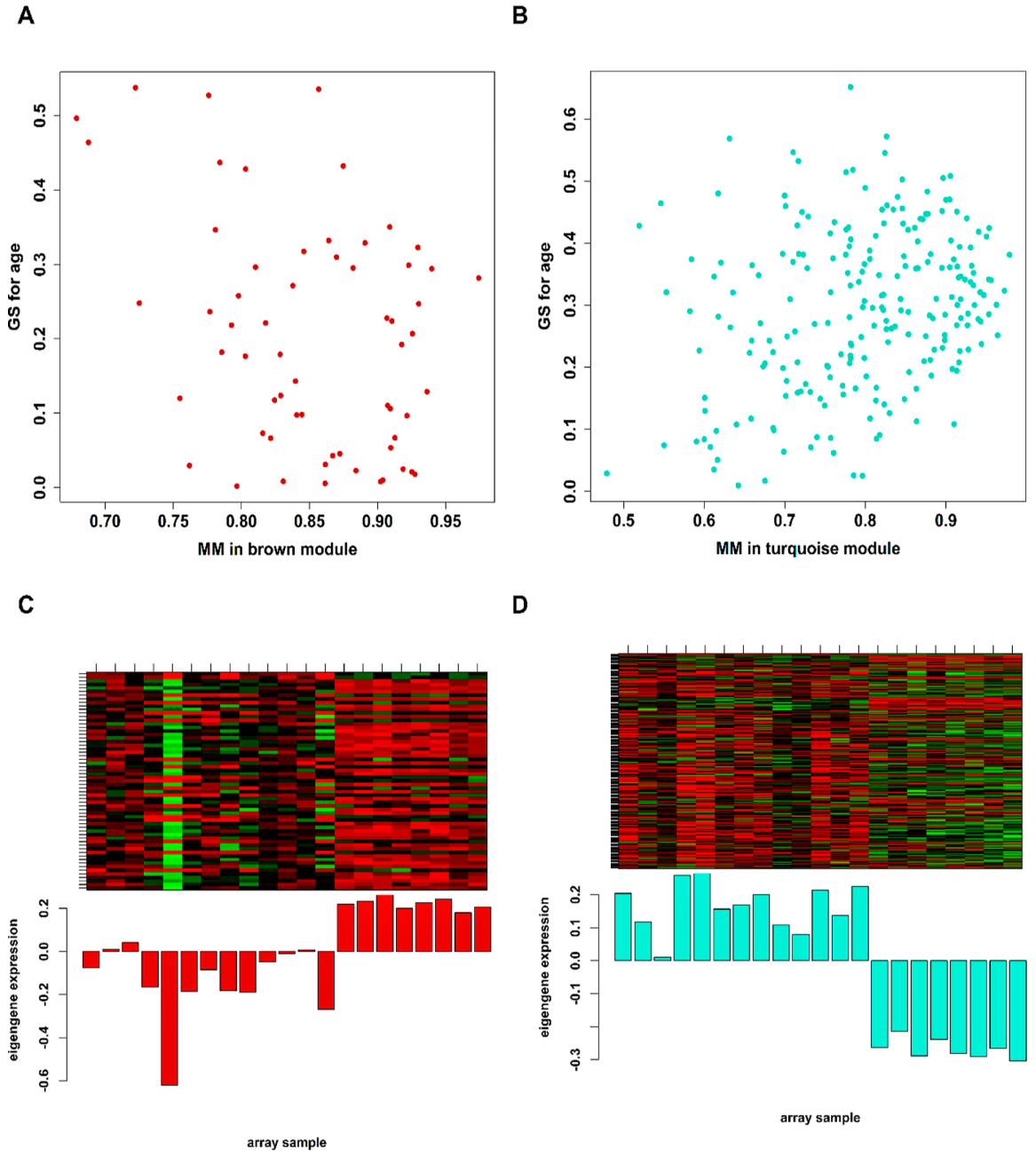

Figure 3. Scatterplot showing significantly ($p < 0.05$) high correlation of GS for age with MM across (A) brown and (B) turquoise modules. Expression heatmap of (C) brown and (D) turquoise community genes, wherein the columns and rows relate to samples and genes. The red- and green-colored bands in the heatmaps signify higher and lower expression levels, respectively. Also, the corresponding ME expression levels (y-axis) across the samples (x-axis) are represented at the base panel of each module heatmap as bar plots.

SFT. The dendrogram and dynamic tree cut algorithm revealed three color-coded modules (i.e., blue, turquoise, and brown) as shown in Figure 2A. The sizes of the modules were as follows: blue = 73, turquoise = 225, and brown = 61. The multi-dimensional scaling (MDS) plot of all modules across 3 scaling dimensions is shown in Figure 2B. Figure 2C shows the GCN as a heatmap plot depicting TOM among the blue, brown, and turquoise module genes. Figure 2D shows a GS Barplot correlated with age, where the turquoise (module significance = 0.29) module was the most favorable followed by brown (module significance = 0.20) and blue (module significance = 0.14). A significantly elevated correlation between GS and MM was noticed in the turquoise (cor = 0.27) and blue (cor = −0.34) modules, respectively.

The correlation values between GS, k.in, and MM along with p-values for all modules are shown in Tables S1−S3. A statistically nonsignificant trend in the blue module based on correlations between GS, MM, and k.in was observed, leading to its immediate elimination. Figure 3A,B displays a GS scatterplot for age concerning MM in brown and turquoise modules. Figure 3C,D shows brown and turquoise module gene heatmaps along with their corresponding ME levels. The turquoise module was the most favorable and highly correlated (module significance = 0.29, GS versus MM = 0.27, GS versus k.in = 0.2, MM versus k.in = 0.99) and was picked as our hub module.

https://doi.org/10.1021/acsomega.3c00020
ACS Omega 2023, 8, 9555−9568

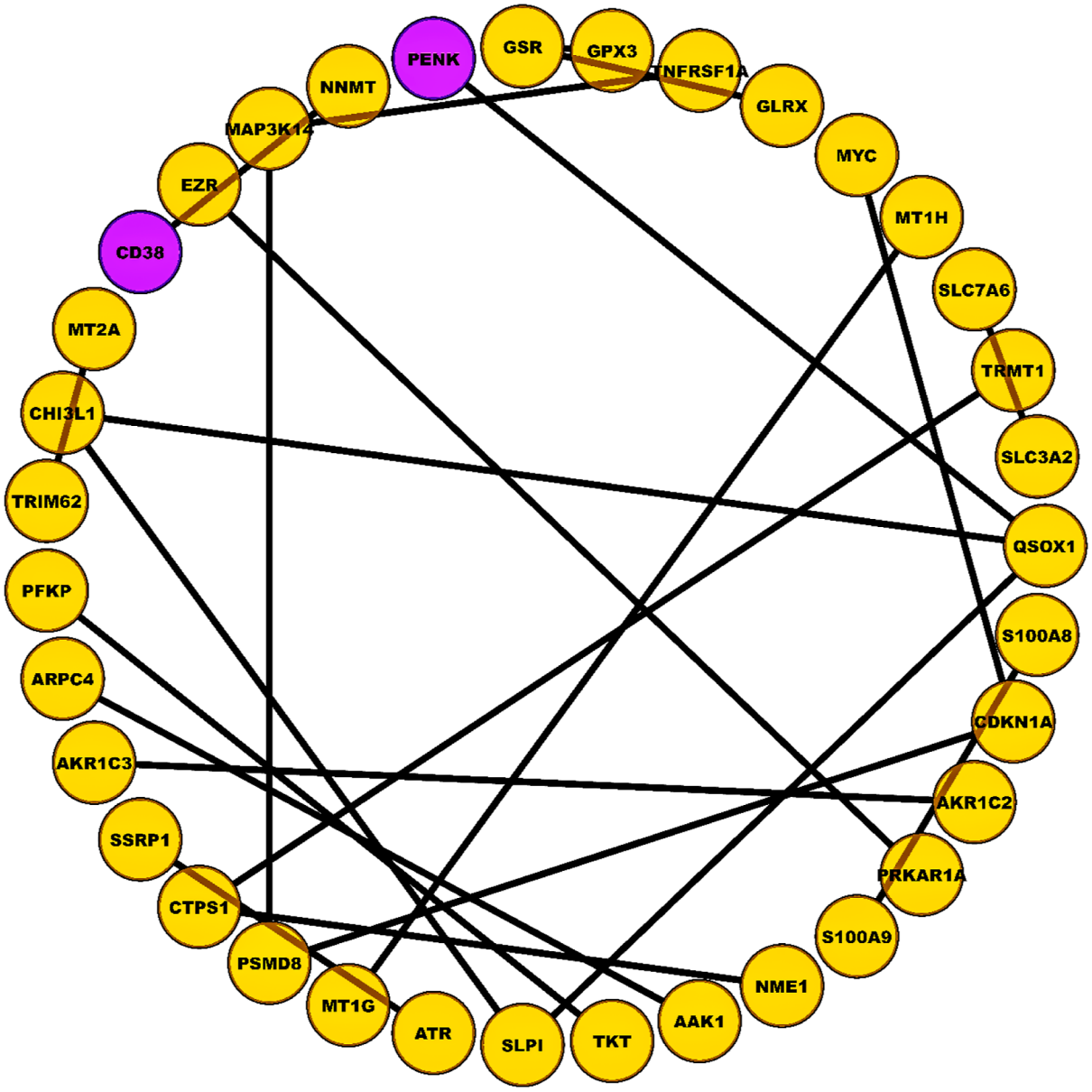

Figure 4. PPI network of hub module comprising 35 nodes and 22 linking edges comparable to a STRING interaction score > 0.9. The yellow- and magenta-colored nodes signify up- and downregulated proteins.

3.3. PPI Network Construction, Pathway, and GO Term Enrichment Analyses. 35 hub module DEGs participated in the PPI network equivalent to a STRING interaction score > 0.9. The PPI network as shown in Figure 4 contains 35 nodes and 22 edges. Among them, 2 were downregulated and 33 were upregulated.

A total of 15 DEGs within our PPI network were involved in the top 5 significant pathways, with nucleotide di- and triphosphate biosynthesis and interconversion (p-value = 2.36×10^{-8}) being the most significant pathway (Table S4). Also, 3 DEGs within our PPI network were involved in the top 5 significantly enriched ontology terms, with hypercortisolism (p-value = 3.08×10^{-4}) being the most significant term (Table S5). PRKAR1A was the overlapping gene between these top 5 significant pathways and GO terms.

3.4. Molecular Docking. For quick screening of the compounds, molecular docking was carried out with the 2992 compounds to the defined binding site of the human PKA RI alpha CNB-B domain (PDB: 5KJX_A) using the LibDock module of Biovia DS2020, which generates 15,2534 conformations of the ligands. For filtering of the hit compounds, consensus scoring was performed in these conformations, and ConfNumber, LibDock score, and Pose number were selected as properties for scoring (Figure 5).

Based on the highest consensus score of 3, 14 compounds were selected as secondary docking using the CDOCKER module of Biovia DS 2020. Finally, 10 hit compounds enlisted in Table S6 were sorted based on -CDOCKER energy, out of which the receptor−ligand interactions of top 3 hit compounds (Bestatin = −50.1402, Buphenine = −35.5733, and ETC-1002 = −35.3644) are shown in Figure 6. These top 3 hit compounds made crucial interactions with the human PKA RI alpha CNB-B domain via active site binding residues, viz., Val283, Val302, Gln304, Val315, Ile327, Ala336, Ala337, Val339, Tyr373, and Asn374.

https://doi.org/10.1021/acsomega.3c00020
ACS Omega 2023, 8, 9555−9568

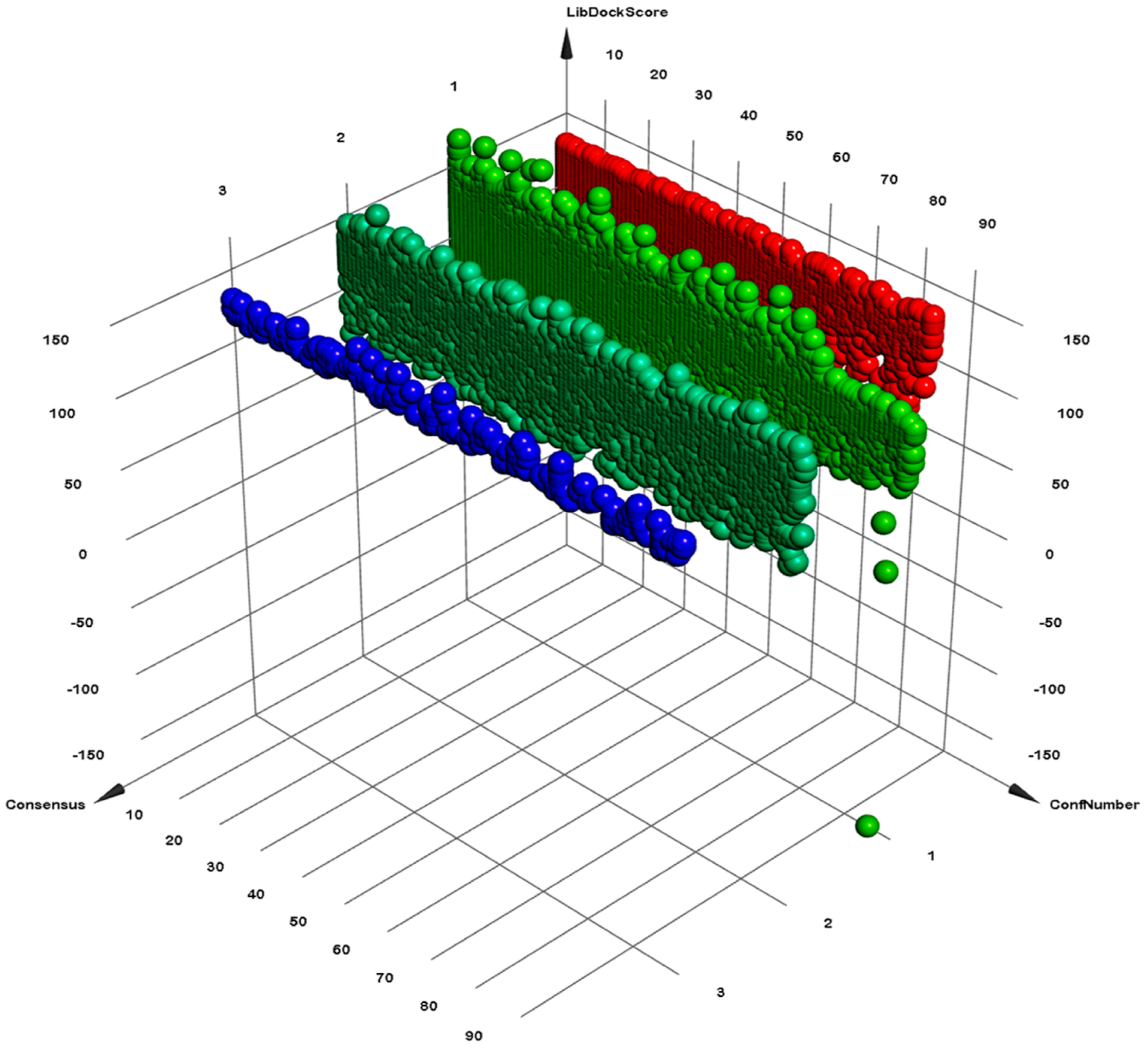

Figure 5. Three-dimensional plot of different conformations of drugs sorted based on the consensus-LibDock score. The red, green, teal, and blue colors represent 0, 1, 2, and 3 consensus scores.

3.5. MD Simulation Analysis. Calculations for RMSD, RMSF, R_g, and intermolecular hydrogen bonds were used to analyze the MD trajectories of the generated simulation run. RMSD is a helpful parameter for examining changes in the protein structure over time. The RMSD analysis identified the protein's backbone fluctuations. The RMSD results showed the time evolution plots of protein backbone deviations during the simulations for all three complexes. Plotting the results through the simulation trajectory and using them to analyze the complex stability is shown in Figure 7A. After 40 ns, the protein backbone's RMSD remained constant, as seen in Figure 7A. The RMSD plot demonstrates that the fluctuations are slightly larger for the topmost compound, S1591. The residual vibrations of a protein molecule can be measured using RMSF during MD simulations. We analyzed the RMSFs of the protein backbone for all systems to look at the flexibility of individual residues (Figure 7B). According to the analysis, the RMSF pattern is consistent across all systems. The plot implies that the protein−ligand complexes are stable because the residual fluctuations are stable. According to the RMSF analysis, the residues in the protein binding pocket that interact with the compounds are essentially stable and only slightly fluctuated throughout the simulation. The tertiary structure of a protein is directly related to R_g, which is the root-mean-square distance of the collection of atoms from their collective center of mass. To examine the protein's compactness in both the apo- and ligand-bound states, the time evolution of R_g was identified. During the simulation, the compactness of each system was assessed. The R_g plot (Figure 7C) indicated that, with the exception of a slight decrease in compound S1591, the protein is stable when the chosen compounds are present. Comparative results indicated that the protein's structural dynamics and folding are consistently stable. To investigate the consistency of hydrogen bonding between the protein−protein and chosen compounds, the intramolecular hydrogen bonds with time were further investigated. In the docked complexes, an estimate of 107

https://doi.org/10.1021/acsomega.3c00020
ACS Omega 2023, 8, 9555−9568

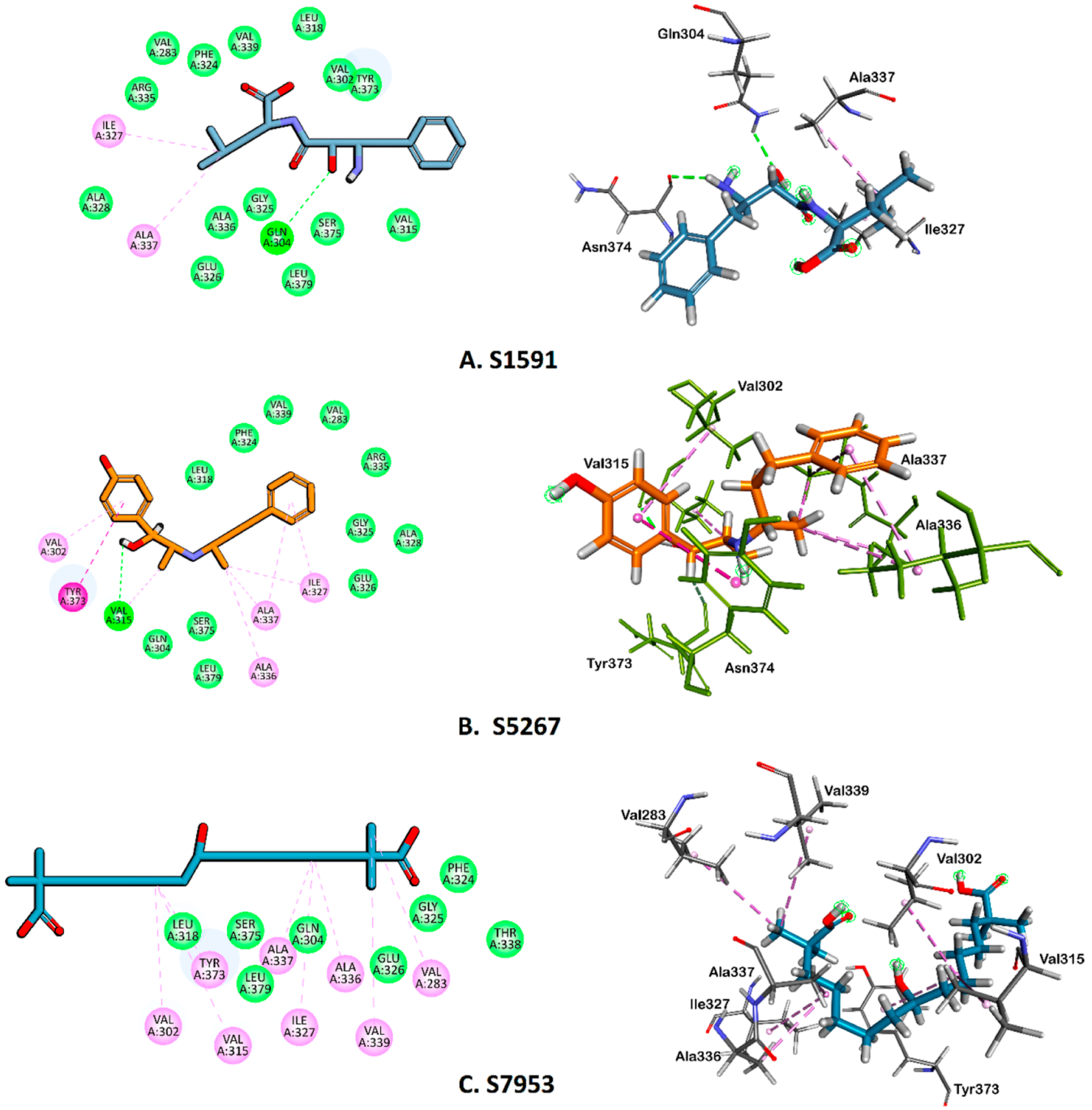

Figure 6. Structure-based virtual screening of small-molecule inhibitors. 2D and 3D schematic representation of the intermolecular interaction of predicted binding modes of A. S1591, B. S5267, and C. S7953.

intramolecular hydrogen bonds in the case of protein−protein and 3−6 intramolecular hydrogen bonds in the case of protein−ligand were made (Figure 7D,E). The analysis showed that, contrary to what the intermolecular hydrogen bonding, which stabilizes the structures, would have predicted, the chosen compounds have not moved from their underlying docking site on the protein.

4. DISCUSSION

Sepsis is a complicated, heterogeneous, and extremely lethal syndrome that may be challenging to perceive and cure.[49] It is described as a life-threatening organ ailment resulting from a dysregulated host reaction to infection.[49] It is anticipated that $>30 \times 10^6$ people worldwide are identified with sepsis every year leading to 5×10^6 fatalities,[50] with excessive financial burden and persistent morbidity among survivors.[51] Sepsis definition has been modified over the previous few decades as our knowledge of it has expanded and its modern-day definition underlines the presence of organ dysfunction.[52] The cornerstone of sepsis-induced organ damage is the discrepancy between tissue perfusion and metabolic demands. Inflammation-induced heart dysfunction and systemic redistribution of blood volume play an important role in this but are exacerbated by tissue oxygen (impaired) utilization.[53]

4.1. Vascular Dysfunction. Many alterations arise concurrently in the systemic vasculature in sepsis patients,

https://doi.org/10.1021/acsomega.3c00020
ACS Omega 2023, 8, 9555−9568

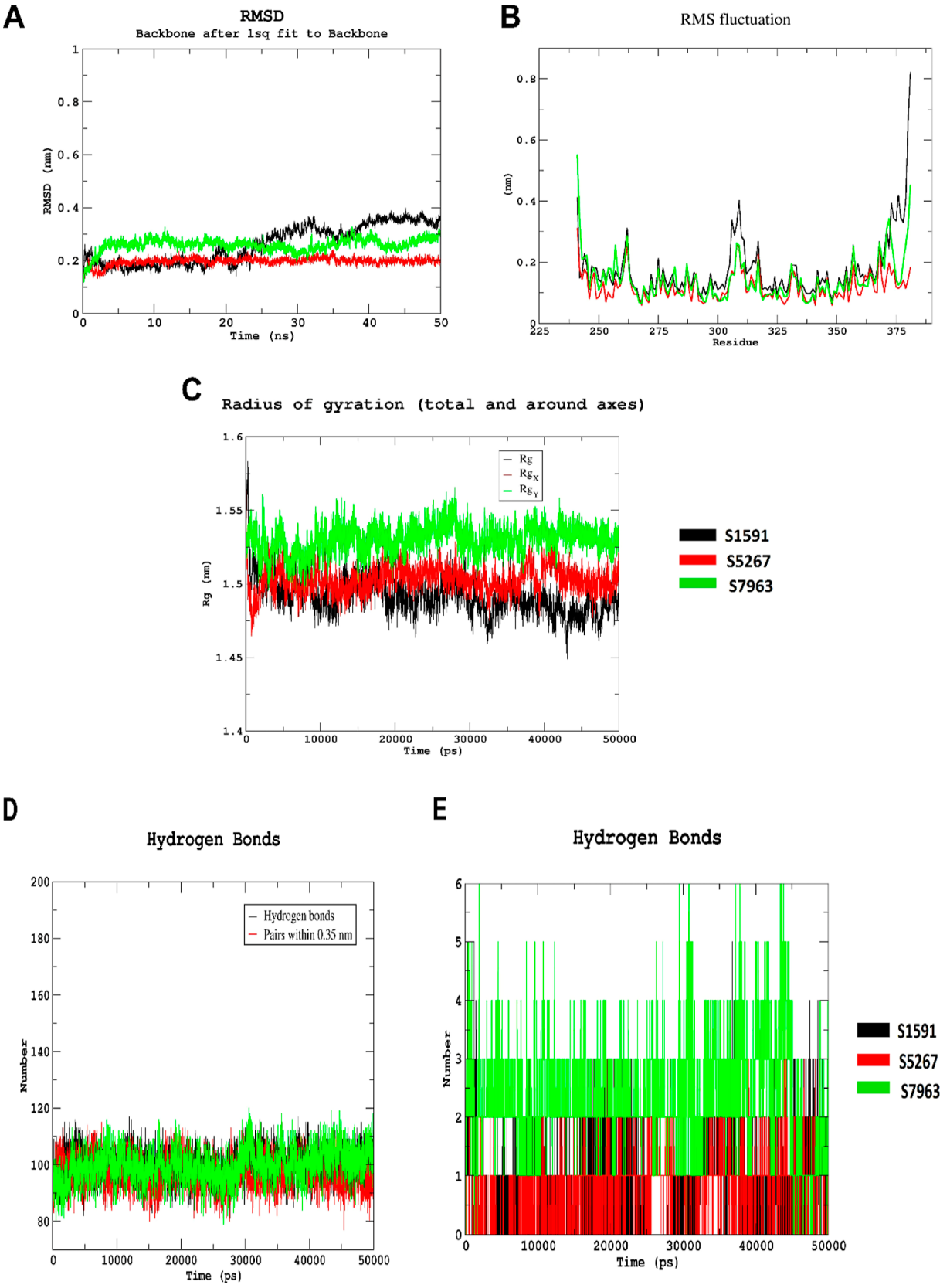

Figure 7. Time-dependent structural dynamics of protein−ligand (PL) complexes: (A) RMSD, (B) RMSF, (C) radius of gyration, (D) intermolecular H-bond between protein and protein, and (E) intermolecular H-bond between protein and ligand.

increasing interest in the significance of microcirculation impairment and dysfunction.[54] Increased capillary permeability lessens efficient systemic perfusion and vascular volume. This paracellular leak appears to be affected by the diffused endothelial damage and dysfunction mediated by pro-inflammatory mediators.[55] In most cases, these anomalies in

https://doi.org/10.1021/acsomega.3c00020
ACS Omega 2023, 8, 9555−9568

volume distribution can be counteracted with successful resuscitation with the sufficient and rational expansion of vascular volumes.[56] Even after reaching a euvolemic state, some patients are accompanied by persistent vasodilation that prevents adequate perfusion. This clinical scenario known as septic shock remains the most severe symptom of sepsis. Vascular smooth muscle finds it difficult to contract under neurohormonal stimulation, developing deep systemic arterial and venous vasodilation, reducing the pressure gradient required for venous return, and resulting in decreased cardiac output.[57,58] The mechanism of this dramatic vascular dysfunction is not understood well, but proinflammatory endothelial dysfunction appears to be related to inducible nitric oxide synthase (iNOS) overexpression.[59] Subsequently, excessive nitric oxide (NO) formation directly induces relaxation and hyperpolarization of smooth muscle cells (vascular), preventing response to vasoconstrictors and prolonging hypotension.[58,60]

4.2. Cardiac Dysfunction. After volume revival and administration of vasopressors, venous return increases and the patient enters a hyper-mechanical profile characterized by elevated cardiac output and lessened systemic vascular resistance.[61] However, these reactions are often accompanied by a decrease in myocardial function. Proinflammatory cytokines like interleukin 1β (IL1β) and interleukin 6 (IL6) induce the expression of vascular cell adhesion molecule 1 (VCAM1) in the coronary endothelium, which inhibits cardiomyocyte contraction and mediates neutrophil infiltration into the myocardium.[25,62] Another important thing is that NO aggravates mitochondrial dysfunction by reducing myocardial oxygen utilization, which prolongs the release of proinflammatory cytokines and downregulates β-adrenergic receptors.[25] Therefore, 1 in 3 patients with sepsis develops left ventricular systolic failure (reversible) due to hypokinesia and decreased ejection fraction with an unclear effect on survival.[63] Sepsis can be linked with incidental clinical cardiac events such as myocardial infarction, heart failure (acute), life-threatening arrhythmias, and myocardial damage (non-ischemic).[64−67]

4.3. Microcirculation and Cellular Dysfunction. Although most therapeutic efforts aim to correct overt hemodynamic dysfunctions, microcirculatory alterations are crucial in sustaining organ damage even after hemodynamic impairment has resolved.[68] Upon injury, endothelial dysfunction and overexpression of iNOS are not uniform in all organ beds, leading to blockage of blood flow and hypoperfusion in some under-expressed tissues.[69] Regardless of proper tissue perfusion or restoration of oxygen delivery, NO interferes with the respiratory chain, inhibiting mitochondrial respiration, resulting in adenosine triphosphate (ATP) depletion, and leading to cellular dysfunction and organ damage.[59,70,71]

4.4. Sepsis Impact on Organs. *4.4.1. Lungs.* The characteristic pathology of the lungs in MODS is a violation of normal gas exchange, manifested primarily in arterial hypoxia. Sepsis is generally considered the most frequent source of acute respiratory distress syndrome (ARDS).[72] ARDS is distinguished by acute respiratory failure, diffused lung infiltration due to alveolar injury, and heightened pulmonary vascular permeability to protein-rich fluids. Although its etiology is not fully understood, studies have shown that the alveolar barrier damage is mediated by pro-inflammatory cytokines such as tumor necrosis factor-alpha (TNFα) or IL1β, which results in widespread endothelial barrier dysfunction and platelet initiation to form microthrombi and the development of neutrophil extracellular traps.[73−75] This edema with alveolar damage, causes a rise in the physiological dead space, impairing gas exchange and leading to severe hypoxemia and hypercapnia.[76] Although the patients benefit from protective ventilator strategies to support inspiratory muscles and maintain sufficient gas exchange,[77] pharmacological interventions to prevent the onset of ARDS or to mitigate its effects on survival have not been successful.[78,79]

4.4.2. Kidneys. The renal system is an additional usual target for this developing organ dysfunction. Sepsis is the most frequent adding factor in acute kidney injury (AKI) in critically ill patients.[80] It occurs in more than half of people with sepsis or septic shock.[81,82] AKI can be described as an increase in serum creatinine of $\geq$0.3 mg/dL over 48 h, 50% above baseline within 7 days, or urine output < 0.5 mL/kg/h for at least 6 h[83] Patients with sepsis-linked AKI have a 62 and 36% higher risk of in-hospital death compared to sepsis patients without AKI.[84] Current evidence indicates a much more key role for local microcirculation and inflammatory signaling (including ischemia-reperfusion injury, oxidative stress, and tubular apoptosis).[85,86] Treatment of sepsis may also contribute to the pathogenesis of AKI using nephrotoxic drugs and excessive or low physiological fluid replacement. Volume overload elevates central venous pressure and raises renal vascular pressure, leading to consequent organ edema, boosted intracapsular pressure, and a decline in glomerular filtration rate.[87,88]

4.4.3. Liver. The liver controls the inflammatory processes and targets host responses. Upon exposure to lipopolysaccharides, Kupffer cells upregulate the release of IL1β, IL6, and TNFα.[89,90] In response to the pro-inflammatory cytokines, hepatocytes release acute phase protein (APP) into the systemic circulation with broad pro- and anti-inflammatory effects.[91] Therefore, it has been suggested that hepatocytes play an important role in stabilizing the immune response in sepsis and preventing excessive inflammatory or immunosuppressive conditions through APP.[90] Hypoxic hepatitis and sepsis-induced cholestasis account for two major mechanisms that explain liver damage and consequent dysfunction in sepsis. Hypoxic hepatitis is usually defined as a clinical condition that is at least 20 times the upper limit of normal serum aminotransferase levels and results in reduced hepatic oxygen delivery or utilization (e.g., cardiac, respiratory, or circulatory failure) without other possible causes of liver damage.[92,93] In sepsis, severe hemodynamic changes, microthrombus formation, sinusoidal obstruction, and endothelial damage disrupt liver perfusion, leading to liver injury and hypoxic hepatitis.[91] Sepsis-induced cholestasis refers to impaired bile production and biliary outflow due to non-obstructive intrahepatic injury[91] and is generally diagnosed when the total serum bilirubin is increased by 2 mg/dL or more and aminotransferase is increased by more than 2 times the maximum normal limit.[94]

For SBVS against FDA-approved medications and analysis, we employed consensus-based LibDock and the CDOCKER module of DS 2020. CDOCKER energy was used to analyze molecules having a higher consensus score in terms of LibDock score and stable conformation. The top 10 compounds were chosen for further research based on these findings. The binding affinity of S1591, S5267, and S7953 with the human PKA RI alpha CNB-B domain was shown to be strong using the CDOCKER module. According to the foregoing findings, these three molecules could be developed and polished into medications.

https://doi.org/10.1021/acsomega.3c00020
ACS Omega 2023, 8, 9555−9568

5. CONCLUSIONS

MODS remain a leading cause of morbidity and mortality particularly in ICU settings with an enormous burden on healthcare resources. Despite all research efforts, therapeutic concepts due to heterogeneity in MODS remain limited and unsatisfactory. Prospective studies are needed to identify robust molecular targets considering disease heterogeneity. In conclusion, through integrated multiomics and in silico methods, we report PRKAR1A as a putative therapeutic target in MODS. Further, we report S1591 (Bestatine), S5267 (Buphenine), and S7953 (ETC-1002) as potent inhibitors for PRKAR1A through the structure-based virtual screening (sbvs) techniques. We propose to conduct experimental validation and evaluate the therapeutic effectiveness of these lead molecules to achieve optimal management of critically ill patients. The molecular target (PRKAR1A), combined with our three lead therapeutic molecules, will guide the accurate therapeutic management in MODS.

■ ASSOCIATED CONTENT

Supporting Information

The Supporting Information is available free of charge at https://pubs.acs.org/doi/10.1021/acsomega.3c00020.

Inclusion and exclusion criteria for dataset selection; plots for assessment of scale-free topology; GS vs MM, GS vs k.in, and MM vs k.in correlation values for all modules; list of top 5 significant pathways and GO terms; and docking scores and drug indication of the top hit compounds (PDF)

■ AUTHOR INFORMATION

Corresponding Author

Ravins Dohare − *Centre for Interdisciplinary Research in Basic Sciences, Jamia Millia Islamia, New Delhi 110025, India;* orcid.org/0000-0002-0602-3719; Email: ravinsdohare@gmail.com

Authors

Prithvi Singh − *Centre for Interdisciplinary Research in Basic Sciences, Jamia Millia Islamia, New Delhi 110025, India*

Mohd Mohsin − *Department of Biotechnology, Faculty of Natural Sciences, Jamia Millia Islamia, New Delhi 110025, India*

Armiya Sultan − *Department of Biotechnology, Faculty of Natural Sciences, Jamia Millia Islamia, New Delhi 110025, India;* orcid.org/0000-0001-5373-8824

Prakash Jha − *Laboratory of Molecular Modeling and Anticancer Drug Development, Dr. B. R. Ambedkar Center for Biomedical Research, University of Delhi, New Delhi 110007, India*

Mohd Mabood Khan − *Department of Zoology, University of Lucknow, Lucknow, Uttar Pradesh 226007, India*

Mansoor Ali Syed − *Department of Biotechnology, Faculty of Natural Sciences, Jamia Millia Islamia, New Delhi 110025, India*

Madhu Chopra − *Laboratory of Molecular Modeling and Anticancer Drug Development, Dr. B. R. Ambedkar Center for Biomedical Research, University of Delhi, New Delhi 110007, India*

Mohammad Serajuddin − *Department of Zoology, University of Lucknow, Lucknow, Uttar Pradesh 226007, India*

Arshad Husain Rahmani − *Department of Medical Laboratories, College of Applied Medical Sciences, Qassim University, Buraydah 51452, Saudi Arabia*

Saleh A. Almatroodi − *Department of Medical Laboratories, College of Applied Medical Sciences, Qassim University, Buraydah 51452, Saudi Arabia*

Faris Alrumaihi − *Department of Medical Laboratories, College of Applied Medical Sciences, Qassim University, Buraydah 51452, Saudi Arabia*

Complete contact information is available at: https://pubs.acs.org/10.1021/acsomega.3c00020

Author Contributions

M.M.: writing—original draft, writing—review & editing. A.S.: writing—original draft, writing—review & editing. P.J.: methodology, software, formal analysis, data curation, writing—original draft, writing—review & editing, visualization. M.M.K.: writing—review & editing. M.A.S.: supervision. M.C.: writing—review & editing. M.S.: writing—review & editing. A.H.R.: writing—review & editing. S.A.A.: writing—review & editing. F.A.: writing—review & editing. R.D.: writing—review & editing, supervision, project administration. P.S.: Conceptualization, methodology, software, formal analysis, data curation, writing—original draft, writing—review & editing, visualization.

Notes

The authors declare no competing financial interest.

The data set used in our study was downloaded from NCBI-GEO under accession number GSE13205 (https://www.ncbi.nlm.nih.gov/geo/query/acc.cgi?acc=GSE13205, accessed on July 10, 2022).

■ ACKNOWLEDGMENTS

The authors would like to thank Jamia Millia Islamia for providing infrastructure, journal access, and internet facilities. M.A.S. would like to thank the Science and Engineering Research Board (SERB), Department of Science and Technology (DST), Government of India, for awarding him Core Research Grant (grant number: CRG/2018/004081). P.S. would like to thank the Indian Council of Medical Research (ICMR) for awarding him Senior Research Fellowship (grant number: BMI/11(89)/2020). M.M. would like to thank SERB, DST, Government of India, for awarding him Junior Research Fellowship (Grant Number: CRG/2018/004081). P.J. would like to thank the DST, Government of India, for awarding him DST-INSPIRE fellowship (grant number: DST/INSPIRE/03/2016/000026). M.C. would like to thank the Department of Biotechnology (DBT), Government of India (grant number: BT/PR40153/BTIS/137/8/2021), for providing Bioinformatics Infrastructure Facility (BIF) at Dr. B. R. Ambedkar Center for Biomedical Research (ACBR).

■ REFERENCES

(1) Singer, M.; Deutschman, C. S.; Seymour, C. W.; Shankar-Hari, M.; Annane, D.; Bauer, M.; Bellomo, R.; Bernard, G. R.; Chiche, J.-D.; Coopersmith, C. M.; Hotchkiss, R. S.; Levy, M. M.; Marshall, J. C.; Martin, G. S.; Opal, S. M.; Rubenfeld, G. D.; van der Poll, T.; Vincent, J.-L.; Angus, D. C. The Third International Consensus Definitions for Sepsis and Septic Shock (Sepsis-3). *JAMA, J. Am. Med. Assoc.* **2016**, *315*, 801.

(2) Hotchkiss, R. S.; Moldawer, L. L.; Opal, S. M.; Reinhart, K.; Turnbull, I. R.; Vincent, J.-L. Sepsis and septic shock. *Nat. Rev. Dis. Prim.* **2016**, *2*, 16045.

(3) Rudd, K. E.; Johnson, S. C.; Agesa, K. M.; Shackelford, K. A.; Tsoi, D.; Kievlan, D. R.; Colombara, D. V.; Ikuta, K. S.; Kissoon, N.; Finfer, S.; Fleischmann-Struzek, C.; Machado, F. R.; Reinhart, K. K.; Rowan, K.; Seymour, C. W.; Watson, R. S.; West, T. E.; Marinho, F.; Hay, S. I.; Lozano, R.; Lopez, A. D.; Angus, D. C.; Murray, C. J. L.; Naghavi, M. Global, Regional, and National Sepsis Incidence and Mortality, 1990-2017: Analysis for the Global Burden of Disease Study. *Lancet* **2020**, *395*, 200−211.
(4) Jarczak, D.; Kluge, S.; Nierhaus, A. Sepsis-Pathophysiology and Therapeutic Concepts. *Front. Med.* **2021**, *8*, 628302.
(5) Schultz, M. J.; Dunser, M. W.; Dunser, A. M.; Dondorp, N. K. J.; Adhikari, S.; Iyer, A.; Kwizera, Y.; Lubell, A.; Papali, L.; Pisani, B. D.; Riviello, D. C.; Angus, L. C.; Azevedo, T.; Baker, J. V.; Diaz, E.; Festic, R.; Haniffa, R.; Jawa, S. T.; Jacob, N.; Kissoon, R.; Lodha, I.; Martin-Loeches, G.; Lundeg, D.; Misango, M.; Mer, S.; Mohanty, S.; Murthy, N.; Musa, J.; Nakibuuka, A.; Serpa Neto, M.; Nguyen Thi Hoang, B.; Nguyen Thien, R.; Pattnaik, J.; Phua, J.; Preller, P.; Povoa, S.; Ranjit, D.; Talmor, J.; Thevanayagam, C. L.; Thwaites, C. L. Current Challenges in the Management of Sepsis in ICUs in Resource-Poor Settings and Suggestions for the Future. *Intensive Care Med.* **2017**, *43*, 612−624.
(6) Rhodes, A.; Evans, L. E.; Alhazzani, W.; Levy, M. M.; Antonelli, M.; Ferrer, R.; Kumar, A.; Sevransky, J. E.; Sprung, C. L.; Nunnally, M. E.; Rochwerg, B.; Rubenfeld, G. D.; Angus, D. C.; Annane, D.; Beale, R. J.; Bellinghan, G. J.; Bernard, G. R.; Chiche, J.-D.; Coopersmith, C.; Backer, D. P.; Fujishima, C. J.; Gerlach, S.; Hidalgo, H.; Hollenberg, J. L.; Jones, S. M.; Karnad, A. E.; Kleinpell, D. R.; Koh, R. M.; Lisboa, Y.; Machado, T. C.; Marini, F. R.; Marshall, J. J.; Mazuski, J. C.; McIntyre, J. E.; McLean, L. A.; Mehta, A. S.; Moreno, S.; Myburgh, R. P.; Navalesi, J.; Nishida, P.; Osborn, O.; Perner, T. M.; Plunkett, A.; Ranieri, C. M.; Schorr, M.; Seckel, C. A.; Seymour, M. A.; Shieh, C. W.; Shukri, L.; Simpson, K. A.; Singer, S. Q.; Thompson, M.; Townsend, B. T.; Van der Poll, S. R.; Vincent, T.; Wiersinga, J.-L.; Zimmerman, W. J.; Dellinger, J. L.; Dellinger, R. P. Surviving Sepsis Campaign: International Guidelines for Management of Sepsis and Septic Shock: 2016. *Intensive Care Med.* **2017**, *43*, 304−377.
(7) Pettilä, V.; Hynninen, M.; Takkunen, O.; Kuusela, P.; Valtonen, M. Predictive Value of Procalcitonin and Interleukin 6 in Critically Ill Patients with Suspected Sepsis. *Intensive Care Med.* **2002**, *28*, 1220−1225.
(8) Morad, E. A.; Rabie, R. A.; Almalky, M. A.; Gebriel, M. G. Evaluation of Procalcitonin, C-Reactive Protein, and Interleukin-6 as Early Markers for Diagnosis of Neonatal Sepsis. *Int. J. Microbiol.* **2020**, *2020*, 8889086.
(9) Velissaris, D.; Pierrakos, C.; Karamouzos, V.; Pantzaris, N. D.; Gogos, C. The Use of Soluble Urokinase Plasminogen Activator Receptor (SuPAR) as a Marker of Sepsis in the Emergency Department Setting. A Current Review. *Acta Clin. Belg.* **2021**, *76*, 79−84.
(10) Zou, Q.; Wen, W.; Zhang, X. Presepsin as a Novel Sepsis Biomarker. *World J. Emerg. Med.* **2014**, *5*, 16.
(11) Chang, W.; Peng, F.; Meng, S.-S.; Xu, J.-Y.; Yang, Y. Diagnostic Value of Serum Soluble Triggering Expressed Receptor on Myeloid Cells 1 (STREM-1) in Suspected Sepsis: A Meta-Analysis. *BMC Immunol.* **2020**, *21*, 2.
(12) Hoffmann, J. J. M. L. Neutrophil CD64 as a Sepsis Biomarker. *Biochem. Med.* **2011**, *21*, 282−290.
(13) Shen, X.; Zhang, J.; Huang, Y.; Tong, J.; Zhang, L.; Zhang, Z.; Yu, W.; Qiu, Y. Accuracy of Circulating MicroRNAs in Diagnosis of Sepsis: A Systematic Review and Meta-Analysis. *J. Intensive Care* **2020**, *8*, 84.
(14) Zhang, W.; Jia, J.; Liu, Z.; Si, D.; Ma, L.; Zhang, G. Circulating MicroRNAs as Biomarkers for Sepsis Secondary to Pneumonia Diagnosed via Sepsis 3.0. *BMC Pulm. Med.* **2019**, *19*, 93.
(15) Wang, W.; Yang, N.; Wen, R.; Liu, C.-F.; Zhang, T.-N. Long Noncoding RNA: Regulatory Mechanisms and Therapeutic Potential in Sepsis. *Front. Cell. Infect. Microbiol.* **2021**, *11*, 563126.
(16) Lee, J.; Banerjee, D. Metabolomics and the Microbiome as Biomarkers in Sepsis. *Crit. Care Clin.* **2020**, *36*, 105−113.
(17) Saito, S.; Uchino, S.; Hayakawa, M.; Yamakawa, K.; Kudo, D.; Iizuka, Y.; Sanui, M.; Takimoto, K.; Mayumi, T.; Sasabuchi, Y. Epidemiology of Disseminated Intravascular Coagulation in Sepsis and Validation of Scoring Systems. *J. Crit. Care* **2019**, *50*, 23−30.
(18) Hotchkiss, R. S.; Monneret, G.; Payen, D. Sepsis-Induced Immunosuppression: From Cellular Dysfunctions to Immunotherapy. *Nat. Rev. Immunol.* **2013**, *13*, 862−874.
(19) Nedeva, C.; Menassa, J.; Puthalakath, H. Sepsis: Inflammation Is a Necessary Evil. *Front. Cell Dev. Biol.* **2019**, *7*, 108.
(20) Hawkins, R. B.; Raymond, S. L.; Stortz, J. A.; Horiguchi, H.; Brakenridge, S. C.; Gardner, A.; Efron, P. A.; Bihorac, A.; Segal, M.; Moore, F. A.; Moldawer, L. L. Chronic Critical Illness and the Persistent Inflammation, Immunosuppression, and Catabolism Syndrome. *Front. Immunol.* **2018**, *9*, 1511.
(21) Hu, Q.; Hao, C.; Tang, S. From Sepsis to Acute Respiratory Distress Syndrome (ARDS): Emerging Preventive Strategies Based on Molecular and Genetic Researches. *Biosci. Rep.* **2020**, *40*, BSR20200830.
(22) Kim, W.-Y.; Hong, S.-B. Sepsis and Acute Respiratory Distress Syndrome: Recent Update. *Tuberc. Respir. Dis.* **2016**, *79*, 53.
(23) Gómez, H.; Kellum, J. A. Sepsis-Induced Acute Kidney Injury. *Curr. Opin. Crit. Care* **2016**, *22*, 546−553.
(24) Mageau, A.; Sacré, K.; Perozziello, A.; Ruckly, S.; Dupuis, C.; Bouadma, L.; Papo, T.; Timsit, J.-F. Septic Shock among Patients with Systemic Lupus Erythematosus: Short and Long-Term Outcome. Analysis of a French Nationwide Database. *J. Infect.* **2019**, *78*, 432−438.
(25) Liu, Y.-C.; Yu, M.-M.; Shou, S.-T.; Chai, Y.-F. Sepsis-Induced Cardiomyopathy: Mechanisms and Treatments. *Front. Immunol.* **2017**, *8*, 1021.
(26) Virzì, G. M.; Clementi, A.; Brocca, A.; de Cal, M.; Marcante, S.; Ronco, C. Cardiorenal Syndrome Type 5 in Sepsis: Role of Endotoxin in Cell Death Pathways and Inflammation. *Kidney Blood Press. Res.* **2016**, *41*, 1008−1015.
(27) Sygitowicz, G.; Sitkiewicz, D. Molecular Mechanisms of Organ Damage in Sepsis: An Overview. *Braz. J. Infect. Dis.* **2020**, *24*, 552−560.
(28) Cao, C.; Yu, M.; Chai, Y. Pathological Alteration and Therapeutic Implications of Sepsis-Induced Immune Cell Apoptosis. *Cell Death Dis.* **2019**, *10*, 782.
(29) Dellinger, R. P.; Carlet, J. M.; Masur, H.; Gerlach, H.; Calandra, T.; Cohen, J.; Gea-Banacloche, J.; Keh, D.; Marshall, J. C.; Parker, M. M.; Ramsay, G.; Zimmerman, J. L.; Vincent, J.-L.; Levy, M. M. Surviving Sepsis Campaign Guidelines for Management of Severe Sepsis and Septic Shock. *Crit. Care Med.* **2004**, *32*, 858−873.
(30) Evans, L.; Rhodes, A.; Alhazzani, W.; Antonelli, M.; Coopersmith, C. M.; French, C.; Machado, F. R.; Mcintyre, L.; Ostermann, M.; Prescott, H. C.; Schorr, C.; Simpson, S.; Wiersinga, W. J.; Alshamsi, F.; Angus, D. C.; Arabi, Y.; Azevedo, L.; Beale, R.; Beilman, G.; Belley-Cote, E.; Burry, L.; Cecconi, M.; Centofanti, J.; Coz Yataco, A.; De Waele, J.; Dellinger, R. P.; Doi, K.; Du, B.; Estenssoro, E.; Ferrer, R.; Gomersall, C.; Hodgson, C.; Hylander Møller, M.; Iwashyna, T.; Jacob, S.; Kleinpell, R.; Klompas, M.; Koh, Y.; Kumar, A.; Kwizera, A.; Lobo, S.; Masur, H.; McGloughlin, S.; Mehta, S.; Mehta, Y.; Mer, M.; Nunnally, M.; Oczkowski, S.; Osborn, T.; Papathanassoglou, E.; Perner, A.; Puskarich, M.; Roberts, J.; Schweickert, W.; Seckel, M.; Sevransky, J.; Sprung, C. L.; Welte, T.; Zimmerman, J.; Levy, M. Surviving Sepsis Campaign: International Guidelines for Management of Sepsis and Septic Shock 2021. *Crit. Care Med.* **2021**, *49*, e1063−e1143.
(31) Luke, D. A.; Harris, J. K. Network Analysis in Public Health: History, Methods, and Applications. *Annu. Rev. Public Health* **2007**, *28*, 69−93.
(32) Xia, X. Bioinformatics and Drug Discovery. *CTMC* **2017**, *17*, 1709−1726.
(33) Zdrazil, B.; Richter, L.; Brown, N.; Guha, R. Moving Targets in Drug Discovery. *Sci. Rep.* **2020**, *10*, 20213.
(34) Berger, S. I.; Iyengar, R. Network Analyses in Systems Pharmacology. *Bioinformatics* **2009**, *25*, 2466−2472.
(35) Cheng, F.; Kovács, I. A.; Barabási, A.-L. Network-Based Prediction of Drug Combinations. *Nat. Commun.* **2019**, *10*, 1197.
(36) Han, Y.; Wang, C.; Klinger, K.; Rajpal, D. K.; Zhu, C. An Integrative Network-Based Approach for Drug Target Indication Expansion. *PLoS One* **2021**, *16*, No. e0253614.

https://doi.org/10.1021/acsomega.3c00020
ACS Omega 2023, 8, 9555−9568

(37) Paananen, J.; Fortino, V. An Omics Perspective on Drug Target Discovery Platforms. *Briefings Bioinf.* **2020**, *21*, 1937−1953.
(38) Clough, E.; Barrett, T. The Gene Expression Omnibus Database. *Methods Mol. Biol.* **2016**, *1418*, 93−110.
(39) Ritchie, M. E.; Phipson, B.; Wu, D.; Hu, Y.; Law, C. W.; Shi, W.; Smyth, G. K. Limma Powers Differential Expression Analyses for RNA-Sequencing and Microarray Studies. *Nucleic Acids Res.* **2015**, *43*, No. e47.
(40) Langfelder, P.; Horvath, S. WGCNA: An R Package for Weighted Correlation Network Analysis. *BMC Bioinf.* **2008**, *9*, 559.
(41) Szklarczyk, D.; Gable, A. L.; Lyon, D.; Junge, A.; Wyder, S.; Huerta-Cepas, J.; Simonovic, M.; Doncheva, N. T.; Morris, J. H.; Bork, P.; Jensen, L. J.; Mering, C. STRING v11: protein-protein association networks with increased coverage, supporting functional discovery in genome-wide experimental datasets. *Nucleic Acids Res.* **2019**, *47*, D607−D613.
(42) Shannon, P.; Markiel, A.; Ozier, O.; Baliga, N. S.; Wang, J. T.; Ramage, D.; Amin, N.; Schwikowski, B.; Ideker, T. Cytoscape: A Software Environment for Integrated Models of Biomolecular Interaction Networks. *Genome Res.* **2003**, *13*, 2498−2504.
(43) Chen, E. Y.; Tan, C. M.; Kou, Y.; Duan, Q.; Wang, Z.; Meirelles, G. V.; Clark, N. R.; Ma'ayan, A. Enrichr: interactive and collaborative HTML5 gene list enrichment analysis tool. *BMC Bioinf.* **2013**, *14*, 128.
(44) Kuleshov, M. V.; Jones, M. R.; Rouillard, A. D.; Fernandez, N. F.; Duan, Q.; Wang, Z.; Koplev, S.; Jenkins, S. L.; Jagodnik, K. M.; Lachmann, A.; McDermott, M. G.; Monteiro, C. D.; Gundersen, G. W.; Ma'ayan, A. Enrichr: A Comprehensive Gene Set Enrichment Analysis Web Server 2016 Update. *Nucleic Acids Res.* **2016**, *44*, W90−W97.
(45) Baby, S. T.; Sharma, S.; Sharma, S.; Enaganti, P. R.; Cherian, R. P. Molecular docking and pharmacophore studies of heterocyclic compounds as Heat shock protein 90 (Hsp90) Inhibitors. *Bioinformation* **2016**, *12*, 149−155.
(46) Lorenz, R.; Moon, E.-W.; Kim, J. J.; Schmidt, S. H.; Sankaran, B.; Pavlidis, I. V.; Kim, C.; Herberg, F. W. Mutations of PKA Cyclic Nucleotide-Binding Domains Reveal Novel Aspects of Cyclic Nucleotide Selectivity. *Biochem. J.* **2017**, *474*, 2389−2403.
(47) Qin, L.; Kuai, J.; Yang, F.; Yang, L.; Sun, P.; Zhang, L.; Li, G. Selected by Bioinformatics and Molecular Docking Analysis, Dhea and 2−14,15-Eg Are Effective against Cholangiocarcinoma. *PLoS One* **2022**, *17*, No. e0260180.
(48) Schüttelkopf, A. W.; van Aalten, D. M. F. *PRODRG* : A Tool for High-Throughput Crystallography of Protein−Ligand Complexes. *Acta Crystallogr., Sect. D: Biol. Crystallogr.* **2004**, *60*, 1355−1363.
(49) Angus, D. C.; van der Poll, T. Severe Sepsis and Septic Shock. *N. Engl. J. Med.* **2013**, *369*, 840−851.
(50) Fleischmann, C.; Scherag, A.; Adhikari, N. K. J.; Hartog, C. S.; Tsaganos, T.; Schlattmann, P.; Angus, D. C.; Reinhart, K.; International Forum of Acute Care Trialists. Assessment of Global Incidence and Mortality of Hospital-Treated Sepsis. Current Estimates and Limitations. *Am. J. Respir. Crit. Care Med.* **2016**, *193*, 259−272.
(51) Tiru, B.; DiNino, E. K.; Orenstein, A.; Mailloux, P. T.; Pesaturo, A.; Gupta, A.; McGee, W. T. The Economic and Humanistic Burden of Severe Sepsis. *Pharmacoeconomics* **2015**, *33*, 925−937.
(52) Caraballo, C.; Jaimes, F. Organ Dysfunction in Sepsis: An Ominous Trajectory From Infection To Death. *Yale J. Biol. Med.* **2019**, *92*, 629−640.
(53) Howell, M. D.; Donnino, M.; Clardy, P.; Talmor, D.; Shapiro, N. I. Occult Hypoperfusion and Mortality in Patients with Suspected Infection. *Intensive Care Med.* **2007**, *33*, 1892−1899.
(54) Hawiger, J.; Veach, R. A.; Zienkiewicz, J. New Paradigms in Sepsis: From Prevention to Protection of Failing Microcirculation. *J. Thromb. Haemostasis* **2015**, *13*, 1743−1756.
(55) Rudiger, A.; Singer, M. Mechanisms of Sepsis-Induced Cardiac Dysfunction. *Crit. Care Med.* **2007**, *35*, 1599−1608.
(56) Guarracino, F.; Bertini, P.; Pinsky, M. R. Cardiovascular Determinants of Resuscitation from Sepsis and Septic Shock. *Crit. Care* **2019**, *23*, 118.
(57) Bloch, A.; Berger, D.; Takala, J. Understanding Circulatory Failure in Sepsis. *Intensive Care Med.* **2016**, *42*, 2077−2079.
(58) Burgdorff, A.-M.; Bucher, M.; Schumann, J. Vasoplegia in Patients with Sepsis and Septic Shock: Pathways and Mechanisms. *J. Int. Med. Res.* **2018**, *46*, 1303−1310.
(59) Morelli, A.; Passariello, M. Hemodynamic Coherence in Sepsis. *Best Pract. Res. Clin. Anaesthesiol.* **2016**, *30*, 453−463.
(60) Barrett, L. K.; Singer, M.; Clapp, L. H. Vasopressin: Mechanisms of Action on the Vasculature in Health and in Septic Shock. *Crit. Care Med.* **2007**, *35*, 33−40.
(61) Rabuel, C.; Mebazaa, A. Septic Shock: A Heart Story since the 1960s. *Intensive Care Med.* **2006**, *32*, 799−807.
(62) Sergi, C.; Shen, F.; Lim, D. W.; Liu, W.; Zhang, M.; Chiu, B.; Anand, V.; Sun, Z. Cardiovascular Dysfunction in Sepsis at the Dawn of Emerging Mediators. *Biomed. Pharmacother.* **2017**, *95*, 153−160.
(63) Sevilla Berrios, R. A.; O'Horo, J. C.; Velagapudi, V.; Pulido, J. N. Correlation of Left Ventricular Systolic Dysfunction Determined by Low Ejection Fraction and 30-Day Mortality in Patients with Severe Sepsis and Septic Shock: A Systematic Review and Meta-Analysis. *J. Crit. Care* **2014**, *29*, 495−499.
(64) Frencken, J. F.; Donker, D. W.; Spitoni, C.; Koster-Brouwer, M. E.; Soliman, I. W.; Ong, D. S. Y.; Horn, J.; van der Poll, T.; van Klei, W. A.; Cremer, M. J. M.; de Beer, O. L.; Bos, L. D. J.; Glas, G. J.; van Hooijdonk, R. T. M.; Schouten, L. R. A.; Straat, M.; Witteveen, E.; Wieske, L.; van Vught, L. A.; Wiewel, M.; Hoogendijk, A. J.; Huson, M. A.; Scicluna, B.; Schultz, M. J.; Klein Klouwenberg, P. M. C.; van de Groep, K.; Verboom, D. Myocardial Injury in Patients With Sepsis and Its Association With Long-Term Outcome. *Circ: Cardiovasc. Qual. Outcomes* **2018**, *11*, No. e004040.
(65) Jafarzadeh, S. R.; Thomas, B. S.; Warren, D. K.; Gill, J.; Fraser, V. J. Longitudinal Study of the Effects of Bacteremia and Sepsis on 5-Year Risk of Cardiovascular Events. *Clin. Infect. Dis.* **2016**, *63*, 495−500.
(66) Shahreyar, M.; Fahhoum, R.; Akinseye, O.; Bhandari, S.; Dang, G.; Khouzam, R. N. Severe sepsis and cardiac arrhythmias. *Ann. Transl. Med.* **2018**, *6*, 6.
(67) Wang, H. E.; Moore, J. X.; Donnelly, J. P.; Levitan, E. B.; Safford, M. M. Risk of Acute Coronary Heart Disease After Sepsis Hospitalization in the REasons for Geographic and Racial Differences in Stroke (REGARDS) Cohort. *Clin. Infect. Dis.* **2017**, *65*, 29−36.
(68) John, J.; Koerber, F.; Schad, M. Differential Discounting in the Economic Evaluation of Healthcare Programs. *Cost Eff. Resour. Allocation* **2019**, *17*, 29.
(69) Ince, C. The Microcirculation Is the Motor of Sepsis. *Crit. Care* **2005**, *9*, S13−S19.
(70) Brealey, D.; Brand, M.; Hargreaves, I.; Heales, S.; Land, J.; Smolenski, R.; Davies, N. A.; Cooper, C. E.; Singer, M. Association between Mitochondrial Dysfunction and Severity and Outcome of Septic Shock. *Lancet* **2002**, *360*, 219−223.
(71) Fink, M. P. Bench-to-Bedside Review: Cytopathic Hypoxia. *Crit. Care* **2002**, *6*, 491−499.
(72) Rubenfeld, G. D.; Caldwell, E.; Peabody, E.; Weaver, J.; Martin, D. P.; Neff, M.; Stern, E. J.; Hudson, L. D. Incidence and Outcomes of Acute Lung Injury. *N. Engl. J. Med.* **2005**, *353*, 1685−1693.
(73) Evans, C. E.; Zhao, Y.-Y. Impact of Thrombosis on Pulmonary Endothelial Injury and Repair Following Sepsis. *Am. J. Physiol.: Lung Cell. Mol. Physiol.* **2017**, *312*, L441−L451.
(74) Matthay, M. A.; Ware, L. B.; Zimmerman, G. A. The Acute Respiratory Distress Syndrome. *J. Clin. Invest.* **2012**, *122*, 2731−2740.
(75) Park, I.; Kim, M.; Choe, K.; Song, E.; Seo, H.; Hwang, Y.; Ahn, J.; Lee, S.-H.; Lee, J. H.; Jo, Y. H.; Kim, K.; Koh, G. Y.; Kim, P. Neutrophils Disturb Pulmonary Microcirculation in Sepsis-Induced Acute Lung Injury. *Eur. Respir. J.* **2019**, *53*, 1800786.
(76) Ranieri, V. M.; Rubenfeld, G. D.; Thompson, B. T.; Ferguson, N. D.; Caldwell, E.; Fan, E.; Camporota, L.; Slutsky, A. S.; ARDS Definition Task Force. Acute Respiratory Distress Syndrome: The Berlin Definition. *JAMA, J. Am. Med. Assoc.* **2012**, *307*, 2526−2533.
(77) Zampieri, F. G.; Mazza, B. Mechanical Ventilation in Sepsis: A Reappraisal. *Shock* **2017**, *47*, 41−46.
(78) Fan, E.; Brodie, D.; Slutsky, A. S. Acute Respiratory Distress Syndrome: Advances in Diagnosis and Treatment. *JAMA, J. Am. Med. Assoc.* **2018**, *319*, 698−710.

https://doi.org/10.1021/acsomega.3c00020
ACS Omega 2023, 8, 9555−9568

(79) Tongyoo, S.; Permpikul, C.; Mongkolpun, W.; Vattanavanit, V.; Udompanturak, S.; Kocak, M.; Meduri, G. U. Hydrocortisone Treatment in Early Sepsis-Associated Acute Respiratory Distress Syndrome: Results of a Randomized Controlled Trial. *Crit. Care* **2016**, *20*, 329.
(80) Bagshaw, S. M.; Uchino, S.; Bellomo, R.; Morimatsu, H.; Morgera, S.; Schetz, M.; Tan, I.; Bouman, C.; Macedo, E.; Gibney, N.; Tolwani, A.; Oudemans-van Straaten, O.; Ronco, C.; Kellum, J. A.; Beginning and Ending Supportive Therapy for the Kidney (BEST Kidney) Investigators. Septic Acute Kidney Injury in Critically Ill Patients: Clinical Characteristics and Outcomes. *Clin. J. Am. Soc. Nephrol.* **2007**, *2*, 431−439.
(81) Poukkanen, M.; Vaara, S. T.; Pettilä, V.; Kaukonen, K.-M.; Korhonen, A.-M.; Hovilehto, S.; Inkinen, O.; LARU-SOMPA, R.; Kaminski, T.; Reinikainen, M.; Lund, V.; Karlsson, S. FINNAKI study group. Acute Kidney Injury in Patients with Severe Sepsis in Finnish Intensive Care Units. *Acta Anaesthesiol. Scand.* **2013**, *57*, 863−872.
(82) Vincent, J.-L.; Sakr, Y.; Sprung, C. L.; Ranieri, V. M.; Reinhart, K.; Gerlach, H.; Moreno, R.; Carlet, J.; Le Gall, J.-R.; Payen, D. Sepsis Occurrence in Acutely Ill Patients Investigators. Sepsis in European Intensive Care Units: Results of the SOAP Study. *Crit. Care Med.* **2006**, *34*, 344−353.
(83) Khwaja, A. KDIGO Clinical Practice Guidelines for Acute Kidney Injury. *Nephron Clin. Pract.* **2012**, *120*, c179−c184.
(84) Bagshaw, S. M.; Lapinsky, S.; Dial, S.; Arabi, Y.; Dodek, P.; Wood, G.; Ellis, P.; Guzman, J.; Marshall, J.; Parrillo, J. E.; Skrobik, Y.; Kumar, A.; Cooperative Antimicrobial Therapy of Septic Shock (CATSS) Database Research Group. Acute Kidney Injury in Septic Shock: Clinical Outcomes and Impact of Duration of Hypotension Prior to Initiation of Antimicrobial Therapy. *Intensive Care Med.* **2009**, *35*, 871−881.
(85) Lerolle, N.; Nochy, D.; Guérot, E.; Bruneval, P.; Fagon, J.-Y.; Diehl, J.-L.; Hill, G. Histopathology of Septic Shock Induced Acute Kidney Injury: Apoptosis and Leukocytic Infiltration. *Intensive Care Med.* **2010**, *36*, 471−478.
(86) Ma, S.; Evans, R. G.; Iguchi, N.; Tare, M.; Parkington, H. C.; Bellomo, R.; May, C. N.; Lankadeva, Y. R. Sepsis-Induced Acute Kidney Injury: A Disease of the Microcirculation. *Microcirculation* **2019**, *26*, No. e12483.
(87) Bellomo, R.; Kellum, J. A.; Ronco, C.; Wald, R.; Martensson, J.; Maiden, M.; Bagshaw, S. M.; Glassford, N. J.; Lankadeva, Y.; Vaara, S. T.; Schneider, A. Acute Kidney Injury in Sepsis. *Intensive Care Med.* **2017**, *43*, 816−828.
(88) Poston, J. T.; Koyner, J. L. Sepsis Associated Acute Kidney Injury. *BMJ* **2019**, *364*, k4891.
(89) Su, G. L. Lipopolysaccharides in Liver Injury: Molecular Mechanisms of Kupffer Cell Activation. *Am. J. Physiol.: Gastrointest. Liver Physiol.* **2002**, *283*, G256−G265.
(90) Yan, J.; Li, S.; Li, S. The Role of the Liver in Sepsis. *Int. Rev. Immunol.* **2014**, *33*, 498−510.
(91) Strnad, P.; Tacke, F.; Koch, A.; Trautwein, C. Liver - Guardian, Modifier and Target of Sepsis. *Nat. Rev. Gastroenterol. Hepatol.* **2017**, *14*, 55−66.
(92) Nesseler, N.; Launey, Y.; Aninat, C.; Morel, F.; Mallédant, Y.; Seguin, P. Clinical Review: The Liver in Sepsis. *Crit. Care* **2012**, *16*, 235.
(93) Waseem, N.; Chen, P.-H. Hypoxic Hepatitis: A Review and Clinical Update. *J. Clin. Transl. Hepatol.* **2016**, *4*, 263−268.
(94) Jenniskens, M.; Langouche, L.; Vanwijngaerden, Y.-M.; Mesotten, D.; Van den Berghe, G. Cholestatic Liver (Dys)Function during Sepsis and Other Critical Illnesses. *Intensive Care Med.* **2016**, *42*, 16−27.

https://doi.org/10.1021/acsomega.3c00020
ACS Omega 2023, 8, 9555−9568